ChinaXiv合作期刊

Anisotropy flows in Pb–Pb collisions at LHC energies from parton scatterings with heavy quark trigger*

Hai Wang[1] and Jin-Hui Chen[1,†]

[1]*Key Laboratory of Nuclear Physics and Ion-beam Application (MOE), Institute of Modern Physics, Fudan University, Shanghai 200433, China*

By implementing an additional heavy quark–antiquark pair production trigger in a multiphase transport (AMPT) model, we study the effect on anisotropy flows of identified particles with a focus on charged particles and quarkonium (J/Ψ and Υ). A systematic increase in the collision rate for active partons in the AMPT model with such an implementation has been observed. It leads to a slight increase of identified particles anisotropy flows as a function of transverse momentum (p_T) and rapidity, and gives a better description of the experimental data of elliptic flow toward larger p_T. Our approach provides an efficient way to study the heavy quark dynamics in the AMPT model at LHC energies.

Keywords: Heavy-ion collision; Quark-Gluon Plasma; Quarkonium; Collective flow

chinaXiv:202201.00065v1

I. INTRODUCTION

In nuclear–nucleus collisions at the Relativistic Heavy Ion Collider (RHIC) and Large Hadron Collider (LHC), a system of color deconfinement, known as Quark-Gluon Plasma (QGP), is expected to be produced [1, 2]. QGP is an almost perfect fluid in the sense that its shear viscosity to entropy density ratio is close to the minimum value [3, 4]. Because the volume and lifetime of the QGP may be much larger and longer than those given by the confinement scale ($\approx 1/\Lambda_{\rm QCD}$), it is expected that the collective flow of partons should arise and have observable consequences that provide information on the dynamics in the QGP [5]. Studies on the anisotropic flow of particle production have contributed significantly to the characterization of the system created at RHIC and LHC [5]. Using a general Fourier series decomposition of the azimuthal distribution of the emitted particles,

$$\frac{{\rm d}N}{{\rm d}\varphi} \propto 1 + 2\sum_{n=1}^{\infty} v_n \cos[n(\varphi - \Psi_n)], \qquad (1)$$

anisotropic flow is quantified using coefficients v_n and the corresponding symmetry planes Ψ_n [6], where φ represents the azimuthal angle of the emitted particles in the momentum space. Systematic measurements of the correlations and fluctuations of v_n coefficients and Ψ_n have been performed in Refs. [7–13]. Comprehensive comparisons with theoretical model calculations provide critical information on the event average initial density distribution in the nuclear overlap region, as well as its connection to QGP dynamics [14–19].

Charm and bottom quarks are important probes for the QGP. They were mainly produced in the initial state of the hard-scattering process prior to QGP formation and survived throughout the evolution stage of the QGP. Quarkonia are bound states of heavy flavor quark–antiquark pairs, which are believed to be suppressed because of the color screening effect in the deconfined interior of the interaction region [20]. They offer a complementary way to study the interaction of the heavy flavor with the medium and, thus, independently shed light on the properties of QGP [21–23]. Dozens of measurements in this direction have been carried out, and rich physical information has been delivered [24–31], with a clear future direction [21].

To study the characteristics of the QGP and its evolution toward chemical and thermal equilibrium, it is necessary to derive transport equations for quarks and gluons when they are in equilibrium and pre-equilibrium [32]. There have been several studies on deriving relativistic abelian and non-abelian transport and constraint equations for the relativistic gauge covariant Wigner operator for color particles interacting via SU(N) gauge fields. This indicates that viscous hydrodynamic models can describe the transverse momentum spectra of light-flavor hadrons and distribution in the azimuthal angle for low $p_{\rm T}$ [16, 33]. On the other hand, transport models have been applied to study the evolution of QGP medium [34]. Owing to its relatively small cross section, a large event sample is required to study charm or even bottom quark transport in the QGP within hydrodynamics calculations or transport model simulations. In this study, we implement an additional heavy quark–antiquark pair production trigger in a multiphase transport (AMPT) model to study the dynamics of charm and bottom quarks in a dense light quark soup. This significantly improves the charm or bottom quark simulation efficiency, and it will be closer to the data at LHC energies because of a large charm quark production cross section [21].

II. TRANSPORT MODELS OF HEAVY FLAVOR

We employed the AMPT model with the string melting version (v2.265) to simulate the collective motion of heavy quarkonium in Pb–Pb collisions at LHC energies. The AMPT model is a hybrid model consisting of fluctuating initial conditions, parton elastic scattering, quark hadronization, and hadronic interaction [34]. It has been used extensively to describe the dynamics of heavy-ion collisions at RHIC and LHC

* This work was supported in part by the Strategic Priority Research Program of the Chinese Academy of Sciences (No. XDB34030200), the Guangdong Major Project of Basic and Applied Basic Research (No. 2020B0301030008), and the National Natural Science Foundation of China (Nos. 12025501, 11890710, 11890714, and 11775288).

† Corresponding author, chenjinhui@fudan.edu.cn

ChinaXiv合作期刊

chinaXiv:202201.00065v1

energies in some recent publications [35–42]. For a detailed description of the AMPT model, please refer to Ref. [34] and Ref. [43] for a summary of recent developments.

In the AMPT model, the initial production of heavy quarks is handled using the HIJING two-component model [44]. It includes pair productions ($q+\bar{q}\to Q+\bar{Q}$, $g+g\to Q+\bar{Q}$) and gluon splitting ($g\to Q+\bar{Q}$) with a cross section in perturbative quantum chromodynamics (QCD) at leading order:

$$\frac{\mathrm{d}\sigma^{Q\bar{Q}}}{\mathrm{d}p_T^2\mathrm{d}y_1\mathrm{d}y_2}=K\sum_{a,b}x_1f_a(x_1,\mu_\mathrm{F}^2)\,x_2f_b(x_2,\mu_\mathrm{F}^2)\times\frac{\mathrm{d}\sigma^{ab\to Q\bar{Q}}}{\mathrm{d}\hat{t}}. \tag{2}$$

Here, y_1 and y_2 are the rapidities of the two produced partons, the K factor aims to account for higher-order corrections of heavy quark production, a and b refer to the types of interacting partons in the initial state, x denotes the nucleon momentum fraction taken by the interaction parton, μ_F represents the factorization scale, f_a is the parton distribution function of parton type a in a nucleon, and $\sigma^{ab\to Q\bar{Q}}$ is the cross section for parton types a and b to produce the heavy quark pair [44]. Because the cross section of heavy quark production, especially for the bottom quark, is several orders of magnitude smaller than that of light quarks in heavy-ion collisions at LHC energies, it calls for a trigger for heavy quark production to increase the simulation efficiency. The algorithm was originally developed by Wang and Gyulassy [44] and was extended to study the bottom quark dynamics in the QGP in this study. We refer to the details in Ref. [44] and Ref. [45] and do not repeat them here.

The final state parton interactions can be described by the equations of motion for the quark and gluon Wigner operators [46, 47], which are closely connected with the classical distribution function. For example, the relativistic gauge covariant Wigner operator for spin-$\frac{1}{2}$ particles in coordinate and momentum space [46]:

$$\hat{W}(\boldsymbol{x},\boldsymbol{p})=\int\frac{\mathrm{d}^4y}{(2\pi)^4}e^{-i\boldsymbol{p}\cdot\boldsymbol{y}}\bar{\psi}(x)\,e^{\frac{1}{2}\boldsymbol{y}\cdot\boldsymbol{D}_{\boldsymbol{x}}^{\dagger}}\otimes e^{-\frac{1}{2}\boldsymbol{y}\cdot\boldsymbol{D}_{\boldsymbol{x}}}\psi(x)\,, \tag{3}$$

where $D^\mu\equiv\partial^\mu+igA^\mu$ is the covariant derivative, and $\hat{W}$ is a matrix in spinor (4×4 components) as well as in the color space ($N\times N$ components).

By using the properties of the link operators, one can derive the quantum transport equation for the QCD Wigner operator [46, 47]. Under semiclassical and Abelian dominance approximations, in the weak-field limit, the equations of motion become a set of equations that resemble classical transport equations [48]. This motivated the study of the final state interaction by solving the Boltzmann equations for quarks and gluons. If only two-body interactions are considered, the Boltzmann equations can be reduced to the following:

$$p^\mu\partial_\mu f(\boldsymbol{x},\boldsymbol{p},t)\propto\int\sigma f(\boldsymbol{x_1},\boldsymbol{p_1},t)f(\boldsymbol{x_2},\boldsymbol{p_2},t), \tag{4}$$

where $f(\boldsymbol{x},\boldsymbol{p},t)$ represents the distribution function of the parton at time t in the phase space, and σ is the cross section for the two-body scattering of partons. Zhang's parton cascade (ZPC) model was developed to study the final-state parton interactions, which solved the Boltzmann equations for partons using the cascade method [48]. In this model, two partons scatter when their closest distance is less than $\sqrt{\sigma/\pi}$. The scattering angle is determined by the differential parton–parton scattering cross section. Because the cascade prescription for solving the semiclassical transport equation does not assume any particular form of the phase space distribution, it can be used to study systems far from local thermal equilibrium, and it automatically takes into account the finite mean free path effect [49]. The current study focuses on heavy quark dynamics at LHC energies, where the bottom quark may be far from thermalization and the charm quark may be close to thermalization [27, 28, 31].

III. RESULTS AND DISCUSSION

To follow the parton scattering history in the AMPT model, we define $N_\mathrm{scat.}$ as the number of two-body elastic scatterings suffered by a parton. The $N_\mathrm{scat.}$ distribution of the active partons ($N_\mathrm{scat.}>0$) is shown in Fig. 1]. The distributions from the AMPT model with an enhanced heavy quark trigger are flatter than those in the normal AMPT calculation, which suggests a larger scattering possibility for partons with enhanced heavy quark triggers in the event. The effect is rather small for the charm quark scenario and more significant for the bottom quark scenario.

Figure 1 also shows the approximate average transverse radial velocity $\langle\beta_\perp\rangle\equiv\langle\hat{\mathbf{r}}_\perp\cdot\hat{\mathbf{p}}_\perp\rangle$ of freeze-out partons with different flavor in the AMPT model as a function of $N_\mathrm{scat.}$, where $\hat{\mathbf{r}}_\perp$ and $\hat{\mathbf{p}}_\perp$ are the transverse radial position and momentum unit vectors. The $\beta_\perp$ is not exactly zero at $N_\mathrm{scat.}=0$ because partons can form only after a finite formation time over which the displacement of a parton depends on its momentum [34]. One sees that $\beta_\perp$ of heavy quarks are larger in magnitude and almost independent of $N_\mathrm{scat.}$, whereas it is smaller in magnitude and drops for light quarks as $N_\mathrm{scat.}$ increases. This is understood because heavy quarks are formed earlier, and they are more likely to inherit the direction of mother partons, which will give them larger $\langle\beta_\perp\rangle$. Compared with light quarks, it is harder to push the heavy quarks away from their original trajectory, their $\langle\beta_\perp\rangle$ are independent of $N_\mathrm{scat.}$. As the mid-rapidity hadron density of a Pb–Pb collision at $\sqrt{s_\mathrm{NN}}=5.02$ TeV reaches as high as a few thousand, depending on the collision centrality [50], triggering on an additional heavy quark–antiquark pair production has a negligible effect on the hadron density, but may affect the evolution dynamics significantly. We use these trigger events to study the properties of QGP matter created in Pb–Pb collisions at LHC energies.

Figure 2 presents v_2, v_3 of a charged hadron in mid-central Pb–Pb collisions at $\sqrt{s_\mathrm{NN}}=5.02$ TeV from AMPT model. To do a fair comparison with experimental data [51], the results are calculated using the two-particle correlation

ChinaXiv合作期刊

chinaXiv:202201.00065v1

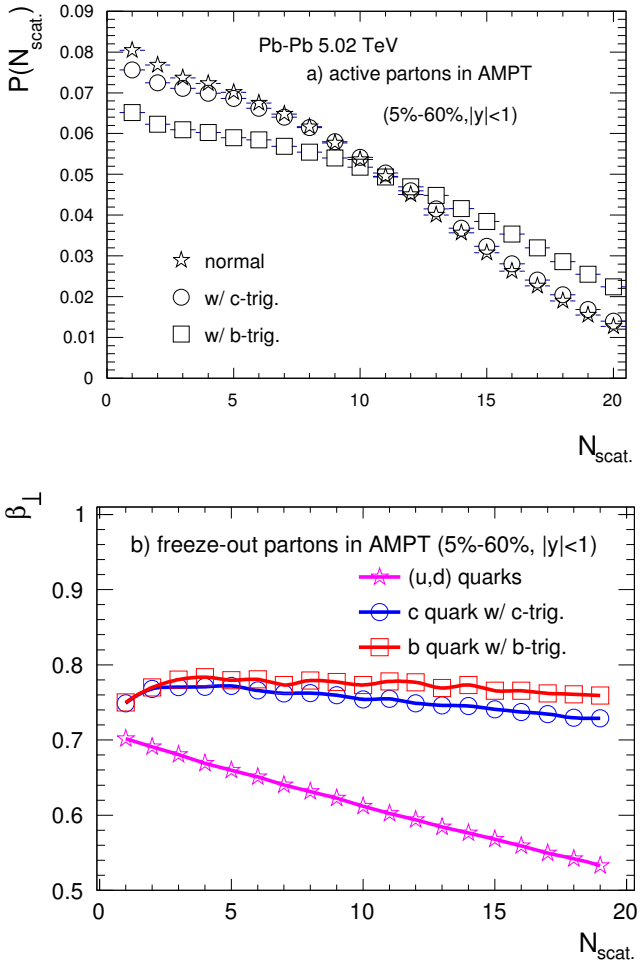

Fig. 1. AMPT simulations of: (a) normalized parton scattering distributions of active quarks; (b) mean transverse velocity of freeze-out quarks in Pb–Pb collisions at $\sqrt{s_{\rm NN}} = 5.02$ TeV and 5%–60% centrality, where normal, w/ c-trig., and w/ b-trig. represent normal AMPT, normal AMPT with triggering an additional charm quark–antiquark pair production, and normal AMPT with triggering an additional bottom quark–antiquark pair production, respectively.

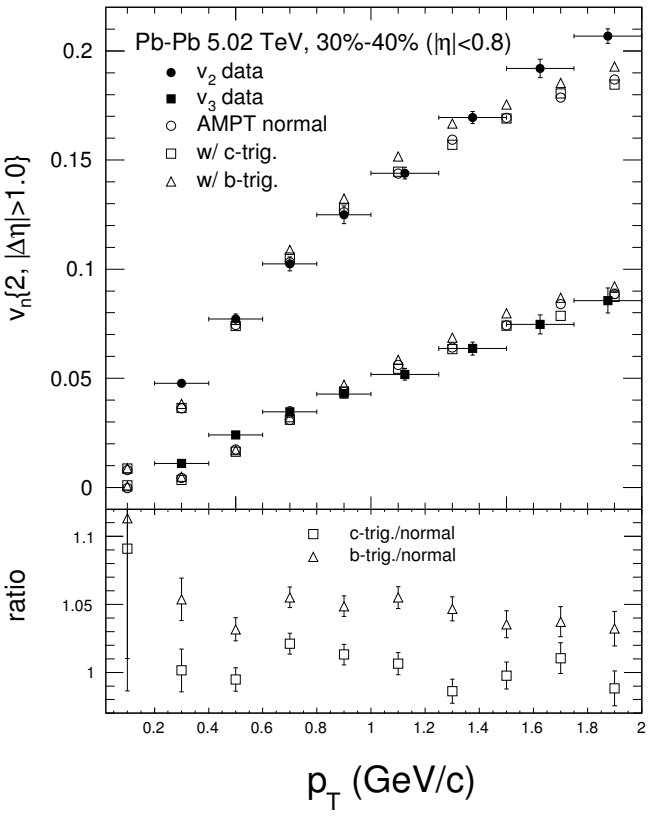

Fig. 2. Charged particles elliptic flow (v_2) and triangular flow (v_3) in mid-central Pb–Pb collisions at $\sqrt{s_{\rm NN}} = 5.02$ TeV from the AMPT model with normal, enhanced heavy quark production trigger settings. The filled points represent experimental data for comparison [51].

method [52]. The result from the reaction plane method, as described in Eq. (1), has been checked and is found to be consistent with Fig. 2. Overall, the AMPT calculations with the normal, enhanced heavy quark trigger scenario reproduce the experimental data reasonably well. Larger elliptic flow is seen in the enhanced heavy quark trigger scenario. The enhancement is approximately 5% and $p_{\rm T}$ independent in AMPT with bottom quark trigger (cf. the bottom panel of Fig. 2). Including the discussion in Fig. 1 where the AMPT model with enhanced bottom quark–antiquark pair production presents a larger scattering possibility for active quarks, which tends to generate larger elliptic flow and is seemingly closer to v_2 data as p_T increases.

Figure 3 highlights the $v_2(p_{\rm T})$ of quarkonia in middle and forward rapidity of Pb–Pb collisions at $\sqrt{s_{\rm NN}} = 5.02$ TeV. The uncertainties in calculations are determined by statistics in different centrality and different rapidity bins. Our results

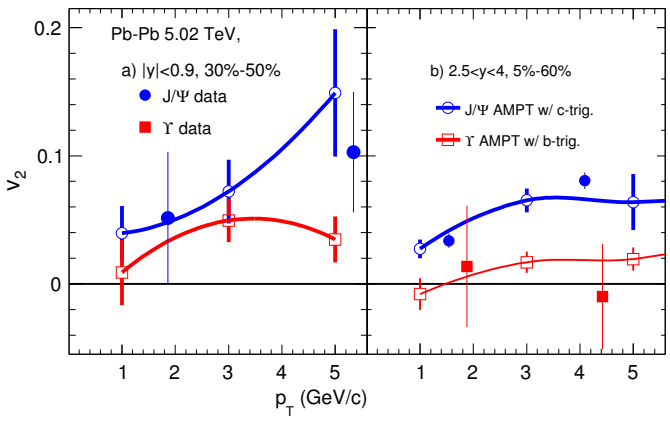

Fig. 3. Heavy flavor quarkonia $v_2(p_T)$ of mid-rapidity and forward rapidity in Pb–Pb collisions at $\sqrt{s_{\rm NN}} = 5.02$ TeV from the AMPT model with enhanced heavy quark–antiquark pair trigger settings. The centralities were chosen to be the same as those in the experimental measurement [31, 53].

ChinaXiv合作期刊

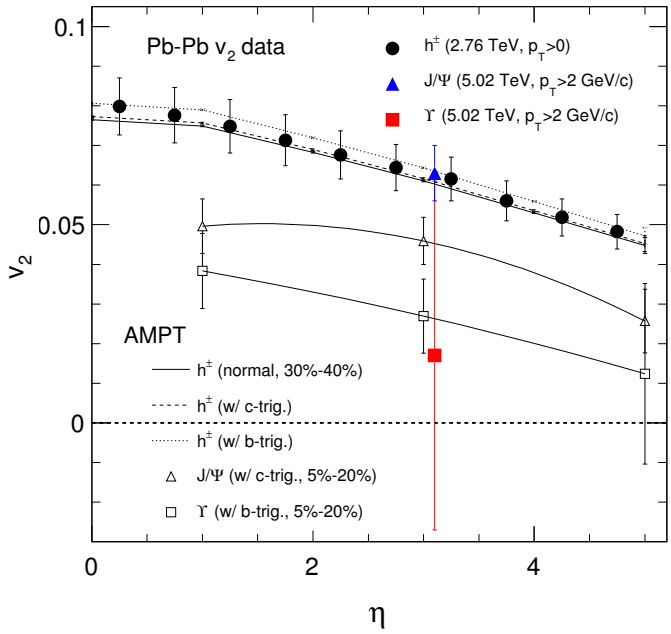

Fig. 4. AMPT model simulations on hadron $v_2(\eta)$ in Pb–Pb collisions at $\sqrt{s_{\rm NN}} = 2.76$ and 5.02 TeV. The centralities and $p_{\rm T}$ bins were chosen to be the same as the experimental data [31, 54]. Different model configurations were applied in the charge hadron calculation, whereas only the heavy quark–antiquark pair trigger settings were used for studying J/Ψ and Υ.

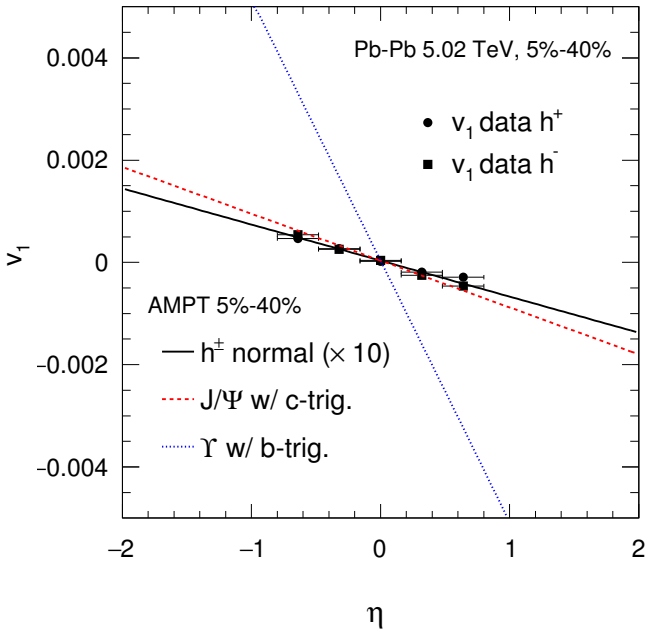

Fig. 5. AMPT model calculations on hadron $v_1(\eta)$ in Pb–Pb collisions at $\sqrt{s_{\rm NN}} = 5.02$ TeV. The charged hadron result is scaled by a factor of 10 for comparison with the experimental data [55].

are consistent with the experimental data considering current uncertainties. Overall, AMPT simulations on v_2 of Υ are smaller than those of J/Ψ. One should note that in the current version of the AMPT calculation, regeneration of J/Ψ or dissociation of Υ are missing, only continued two-body elastic scattering is involved, which seems to generate the finite v_2 of quarkonia. The magnitude difference between Υ and J/Ψ may be due to the mass of different quarks associated with each calculation. We have learned that it is also one of the key parameters in hydrodynamics calculations [16, 33].

To study this further, we examined the differential rapidity (pseudorapidity) dependence on v_2, as shown in Fig. 4. Because $v_2(\eta)$ data for a charged hadron in Pb–Pb collisions at $\sqrt{s_{NN}} = 5.02$ TeV has not yet been published, we chose the data [54] at $\sqrt{s_{\rm NN}} = 2.76$ TeV for comparison. Thus, the AMPT calculation for the charged hadron is performed on $\sqrt{s_{\rm NN}} = 2.76$ TeV accordingly. Our calculations with normal or enhanced heavy quark–antiquark pair production scenarios describe the data fairly well. Although the uncertainties presented in the measurement do not allow us to distinguish between different scenarios, the difference in the calculations is of a few per cent. The value of Υ v_2 is positive and at a maximum at mid-rapidity, and close to zero at higher rapidity. The calculation appears to agree with the data at forward rapidity [31]. The value of J/Ψ v_2 is larger than Υ and exhibits similar rapidity dependence. However, it underpredicts the data at forward rapidity. This deviation may originate from the missing dissociation and regeneration mechanisms for heavy quarkonium in the AMPT. Further studies are required to implement these effects in the AMPT model.

The enhanced heavy quark–antiquark pair production event can also be applied to study the direct flow (v_1) of quarkonium. This represents a new probe for studying the strong electromagnetic field effect of hot QCD matter via v_1 measurement, particularly on the difference in $v_1(\eta)$ between the particle and its antiparticle [56–58]. Measurements of the open charm meson $v_1(\eta)$ show a difference in the slopes of D^0 and $\bar{D}^0$, but with a different sign from RHIC to LHC [55, 59, 60]. The origin of this physics is still debated. Because the electromagnetic field effect has not been implemented in the AMPT model, we consider the $v_1(\eta)$ of J/Ψ and Υ instead of the v_1 difference between the particle and antiparticle in our current framework. In this aspect, we used the coordinate system of the model with the x-axis along the impact parameter direction ($\vec{b}$) of each event in the transverse plane, with the center of the projective and target nuclei at the transverse coordinates $(b/2, 0)$ and $(-b/2, 0)$. The direction of the projectile momentum specifies the z-axis; consequently, the total angular momentum of the system is along the $-y$ direction. Figure 5 shows our results for J/Ψ and Υ together with the charged hadron in Pb–Pb collisions at $\sqrt{s_{\rm NN}} = 5.02$ TeV. It can be seen that quarkonia present an order of magnitude larger $v_1(\eta)$ than charged hadrons, presumably because of the early formation and larger mass. In comparison with the data [55], the $v_1(\eta)$ of the charged hadron from the AMPT model is on the correct sign but an order of magnitude lower. Because the dynamics that gener-

chinaXiv:202201.00065v1

ChinaXiv合作期刊

ates v_1 is quite complicated, it may depend on the equation of state, mean-field potentials, particle scattering, shadowing from spectator nucleons, and tilt of the hot dense QCD matter in the x–z plane [58]. Our results rely on two-body parton elastic scattering, and naive quark hadronization can be understood. Future studies with more realistic dynamics are of interest.

IV. SUMMARY

In summary, we have implemented an additional heavy flavor quark–antiquark pair production trigger in the AMPT model to study their dynamics in hot and dense media created in high-energy heavy-ion collisions. In this study, we have focused on the heavy flavor quarkonium anisotropy flows in Pb–Pb collisions at LHC energies. The new implementation presents a systematic increase in the flow coefficients as a function of $p_{\rm T}$ and η in comparison with the result from the normal AMPT model and provides an efficient way to study quarkonium dynamics with relatively small event samples. It describes the charged particle, J/Ψ, and Υ v_2 reasonably well. Future efforts are required to include more realistic dynamics in the AMPT model, such as the dissociation and regeneration of heavy quarkonium production at LHC energies.

ACKNOWLEDGMENTS

Discussions with Dr. Hui Li are gratefully acknowledged.

AUTHOR CONTRIBUTIONS

All authors contributed to the study conception and design. Material preparation, data collection and analysis were performed by Hai Wang and Jinhui Chen. The first draft of the manuscript was written by Hai Wang and Jin-Hui Chen, and all authors commented on previous versions of the manuscript. All authors read and approved the final manuscript.

[1] K. Yagi, T. Hatsuda, Y. Miake, Quark-gluon plasma: From big bang to little bang. Camb. Univ. Press. ISBN -10: 0521561086,.

[2] J. Chen, D. Keane, Y.G. Ma, et al., Antinuclei in Heavy-Ion Collisions. Phys. Rept. **760**, 1–39 (2018). doi:10.1016/j.physrep.2018.07.002

[3] P. Kovtun, D.T. Son, A.O. Starinets, Viscosity in strongly interacting quantum field theories from black hole physics. Phys. Rev. Lett. **94**, 111601 (2005). doi:10.1103/PhysRevLett.94.111601

[4] N. Demir, S.A. Bass, Shear-Viscosity to Entropy-Density Ratio of a Relativistic Hadron Gas. Phys. Rev. Lett. **102**, 172302 (2009). doi:10.1103/PhysRevLett.102.172302

[5] U. Heinz, R. Snellings, Collective flow and viscosity in relativistic heavy-ion collisions. Ann. Rev. Nucl. Part. Sci. **63**, 123–151 (2013). doi:10.1146/annurev-nucl-102212-170540

[6] S.A. Voloshin, A.M. Poskanzer, R. Snellings, Collective phenomena in non-central nuclear collisions. Landolt-Bornstein **23**, 293–333 (2010). doi:10.1007/978-3-642-01539-7_10

[7] C. Adler, Z. Ahammed, C. Allgower, et al., Elliptic flow from two and four particle correlations in Au+Au collisions at s(NN)**(1/2) = 130-GeV. Phys. Rev. C **66**, 034904 (2002). doi:10.1103/PhysRevC.66.034904

[8] B. Alver, B.B. Back, M.D.o. Baker, Importance of correlations and fluctuations on the initial source eccentricity in high-energy nucleus-nucleus collisions. Phys. Rev. C **77**, 014906 (2008). doi:10.1103/PhysRevC.77.014906

[9] B.I. Abelev, M.M. Aggarwal, Z. Ahammed, et al., Centrality dependence of charged hadron and strange hadron elliptic flow from s(NN)**(1/2) = 200-GeV Au + Au collisions. Phys. Rev. C **77**, 054901 (2008). doi:10.1103/PhysRevC.77.054901

[10] S. Afanasiev, C. Aidala, N.N.o. Ajitanand, Systematic Studies of Elliptic Flow Measurements in Au+Au Collisions at s**(1/2) = 200-GeV. Phys. Rev. C **80**, 024909 (2009). doi:10.1103/PhysRevC.80.024909

[11] S. Chatrchyan, V. Khachatryan, A.M. Sirunyan, et al., Measurement of the elliptic anisotropy of charged particles produced in PbPb collisions at $\sqrt{s_{NN}}$=2.76 TeV. Phys. Rev. C **87**, 014902 (2013). doi:10.1103/PhysRevC.87.014902

[12] G. Aad, B. Abbott, J. Abdallah, et al., Measurement of event-plane correlations in $\sqrt{s_{NN}}$ = 2.76 TeV lead-lead collisions with the ATLAS detector. Phys. Rev. C **90**, 024905 (2014). doi:10.1103/PhysRevC.90.024905

[13] S. Acharya, F. Acosta, D.o. Adamova, Energy dependence and fluctuations of anisotropic flow in Pb-Pb collisions at $\sqrt{s_{\rm NN}}$ = 5.02 and 2.76 TeV. JHEP **07**, 103 (2018). doi:10.1007/JHEP07(2018)103

[14] K. Dusling, W. Li, B. Schenke, Novel collective phenomena in high-energy proton–proton and proton–nucleus collisions. Int. J. Mod. Phys. E **25**, 1630002 (2016). doi:10.1142/S0218301316300022

[15] J.L. Nagle, W.A. Zajc, Small System Collectivity in Relativistic Hadronic and Nuclear Collisions. Ann. Rev. Nucl. Part. Sci. **68**, 211–235 (2018). doi:10.1146/annurev-nucl-101916-123209

[16] C. Shen, L. Yan, Recent development of hydrodynamic modeling in heavy-ion collisions. Nucl. Sci. Tech. **31**, 122 (2020). doi:10.1007/s41365-020-00829-z

[17] S. Wu, C. Shen, H. Song, Dynamical exploring the QCD matter at finite temperatures and densities-a short review. Chin. Phys. Lett. **38**, 081201 (2021). doi:10.1088/0256-307X/38/8/081201

[18] Z. Han, B. Chen, Y. Liu, Critical temperature of deconfinement in a constrained space using a bag model at vanishing baryon density. Chin. Phys. Lett. **37**, 112501 (2020). doi:10.1088/0256-307X/37/11/112501

[19] R.H. Fang, R.D. Dong, D.F. Hou, et al., Thermodynamics of the system of massive Dirac fermions in a uniform magnetic field. Chin. Phys. Lett. **38**, 091201 (2021). doi:10.1088/0256-307X/38/9/091201

[20] T. Matsui, H. Satz, J/ψ Suppression by Quark-Gluon Plasma Formation. Phys. Lett. B **178**, 416–422 (1986).

chinaXiv:202201.00065v1

ChinaXiv合作期刊

chinaXiv:202201.00065v1

doi:10.1016/0370-2693(86)91404-8

[21] N. Brambilla, S. Eidelman, B. Heltsley, et al., Heavy Quarkonium: Progress, Puzzles, and Opportunities. Eur. Phys. J. C **71**, 1534 (2011). doi:10.1140/epjc/s10052-010-1534-9

[22] Z.B. Tang, W.M. Zha, Y.F. Zhang, An experimental review of open heavy flavor and quarkonium production at RHIC. Nucl. Sci. Tech. **31**, 81 (2020). doi:10.1007/s41365-020-00785-8

[23] J. Zhao, K. Zhou, S. Chen, et al., Heavy flavors under extreme conditions in high energy nuclear collisions. Prog. Part. Nucl. Phys. **114**, 103801 (2020). doi:10.1016/j.ppnp.2020.103801

[24] A. Adare, S. Afanasiev, C. Aidala, et al., J/ψ Production vs Centrality, Transverse Momentum, and Rapidity in Au+Au Collisions at $\sqrt{s_{NN}} = 200$ GeV. Phys. Rev. Lett. **98**, 232301 (2007). doi:10.1103/PhysRevLett.98.232301

[25] R. Aaij, B. Adeva, M. Adinolfi, et al., Study of Υ production and cold nuclear matter effects in pPb collisions at $\sqrt{s_{NN}}$=5 TeV. JHEP **07**, 094 (2014). doi:10.1007/JHEP07(2014)094

[26] L. Adamczyk, J.K. Adkins, G. Agakishiev, et al., Energy dependence of J/ψ production in Au+Au collisions at $\sqrt{s_{NN}} =$ 39, 62.4 and 200 GeV. Phys. Lett. B **771**, 13–20 (2017). doi:10.1016/j.physletb.2017.04.078

[27] V. Khachatryan, et al., Suppression of $\Upsilon(1S), \Upsilon(2S)$ and $\Upsilon(3S)$ production in PbPb collisions at $\sqrt{s_{\rm NN}}$ = 2.76 TeV. Phys. Lett. B **770**, 357–379 (2017). doi:10.1016/j.physletb.2017.04.031

[28] M. Aaboud, G. Aad, B. Abbott, et al., Prompt and non-prompt J/ψ and $\psi(2S)$ suppression at high transverse momentum in 5.02 TeV Pb+Pb collisions with the ATLAS experiment. Eur. Phys. J. C **78**, 762 (2018). doi:10.1140/epjc/s10052-018-6219-9

[29] M. Aaboud, A. G., B. Abbott, et al., Measurement of quarkonium production in proton–lead and proton–proton collisions at 5.02 TeV with the ATLAS detector. Eur. Phys. J. C **78**, 171 (2018). doi:10.1140/epjc/s10052-018-5624-4

[30] J. Adam, et al., Measurement of inclusive J/ψ suppression in Au+Au collisions at $\sqrt{s_{NN}}$ = 200 GeV through the dimuon channel at STAR. Phys. Lett. B **797**, 134917 (2019). doi:10.1016/j.physletb.2019.134917

[31] S. Acharya, D. Adamová, S.P. Adhya, et al., Measurement of $\Upsilon(1S)$ elliptic flow at forward rapidity in Pb-Pb collisions at $\sqrt{s_{\rm NN}} = 5.02$ TeV. Phys. Rev. Lett. **123**, 192301 (2019). doi:10.1103/PhysRevLett.123.192301

[32] B.I. Abelev, et al., Observation of an Antimatter Hypernucleus. Sci. **328**, 58–62 (2010). doi:10.1126/science.1183980

[33] B. Schenke, S. Jeon, C. Gale, (3+1)D hydrodynamic simulation of relativistic heavy-ion collisions. Phys. Rev. C **82**, 014903 (2010). doi:10.1103/PhysRevC.82.014903

[34] Z.W. Lin, C.M. Ko, B.A. Li, et al., A Multi-phase transport model for relativistic heavy ion collisions. Phys. Rev. C **72**, 064901 (2005). doi:10.1103/PhysRevC.72.064901

[35] C. Zhang, Z.W. Lin, Left-right splitting of elliptic flow due to directed flow in heavy ion collisions. . arXiv:2109.04987

[36] D. Shen, J. Chen, Z.W. Lin, The effect of hadronic scatterings on the measurement of vector meson spin alignments in heavy-ion collisions. Chin. Phys. C **45**, 054002 (2021). doi:10.1088/1674-1137/abe763

[37] L. Zheng, G.H. Zhang, Y.F. Liu, et al., Investigating high energy proton proton collisions with a multi-phase transport model approach based on PYTHIA8 initial conditions. Eur. Phys. J. C **81**, 755 (2021). doi:10.1140/epjc/s10052-021-09527-5

[38] C.Z. Wang, W.Y. Wu, Q.Y. Shou, et al., Interpreting the charge-dependent flow and constraining the chiral magnetic wave with event shape engineering. Phys. Lett. B **820**, 136580 (2021). doi:10.1016/j.physletb.2021.136580

[39] H. Wang, J. Chen, Study on open charm hadron production and angular correlation in high-energy nuclear collisions. Nucl. Sci. Tech. **32**, 2 (2021). doi:10.1007/s41365-020-00839-x

[40] X.L. Zhao, G.L. Ma, Y.G. Ma, et al., Validation and improvement of the ZPC parton cascade inside a box. Phys. Rev. C **102**, 024904 (2020). doi:10.1103/PhysRevC.102.024904

[41] T. Shao, J. Chen, C.M. Ko, et al., Enhanced production of strange baryons in high-energy nuclear collisions from a multiphase transport model. Phys. Rev. C **102**, 014906 (2020). doi:10.1103/PhysRevC.102.014906

[42] C. Zhang, L. Zheng, F. Liu, et al., Update of a multiphase transport model with modern parton distribution functions and nuclear shadowing. Phys. Rev. C **99**, 064906 (2019). doi:10.1103/PhysRevC.99.064906

[43] Z.W. Lin, L. Zheng, Further developments of a multi-phase transport model for relativistic nuclear collisions. Nucl. Sci. Tech. **32**, 113 (2021). doi:10.1007/s41365-021-00944-5

[44] X.N. Wang, M. Gyulassy, HIJING: A Monte Carlo model for multiple jet production in p p, p A and A A collisions. Phys. Rev. D **44**, 3501–3516 (1991). doi:10.1103/PhysRevD.44.3501

[45] H. Wang, J. Chen, Y.G. Ma, et al., Charm hadron azimuthal angular correlations in au+ au collisions at $sqrts_NN = 200$ gev from parton scatterings. Nucl. Sci. Tech. **30**, 185 (2019). doi:https://doi.org/10.1007/s41365-019-0706-z

[46] H.T. Elze, M. Gyulassy, D. Vasak, Transport Equations for the QCD Quark Wigner Operator. Nucl. Phys. B **276**, 706–728 (1986). doi:10.1016/0550-3213(86)90072-6

[47] H.T. Elze, M. Gyulassy, D. Vasak, Transport Equations for the QCD Gluon Wigner Operator. Phys. Lett. B **177**, 402–408 (1986). doi:10.1016/0370-2693(86)90778-1

[48] B. Zhang, ZPC 1.0.1: A Parton cascade for ultrarelativistic heavy ion collisions. Comput. Phys. Commun. **109**, 193–206 (1998). doi:10.1016/S0010-4655(98)00010-1

[49] B. Zhang, M. Gyulassy, C.M. Ko, Elliptic flow from a parton cascade. Phys. Lett. B **455**, 45–48 (1999). doi:10.1016/S0370-2693(99)00456-6

[50] J. Adam, D. Adamová, M.M. Aggarwal, et al., Centrality dependence of the charged-particle multiplicity density at midrapidity in Pb-Pb collisions at $\sqrt{s_{\rm NN}}$ = 5.02 TeV. Phys. Rev. Lett. **116**, 222302 (2016). doi:10.1103/PhysRevLett.116.222302

[51] J. Adam, D. Adamová, M.M. Aggarwal, et al., Anisotropic flow of charged particles in Pb-Pb collisions at $\sqrt{s_{\rm NN}} = 5.02$ TeV. Phys. Rev. Lett. **116**, 132302 (2016). doi:10.1103/PhysRevLett.116.132302

[52] L.Y. Zhang, J.H. Chen, Z.W. Lin, et al., Two-particle angular correlations in pp and p-Pb collisions at energies available at the CERN Large Hadron Collider from a multiphase transport model. Phys. Rev. C **98**, 034912 (2018). doi:10.1103/PhysRevC.98.034912

[53] S. Acharya, S. Acharya, D. Adamova, et al., J/ψ elliptic and triangular flow in Pb-Pb collisions at $\sqrt{s_{\rm NN}}$ = 5.02 TeV. JHEP **10**, 141 (2020). doi:10.1007/JHEP10(2020)141

[54] J. Adam, et al., Pseudorapidity dependence of the anisotropic flow of charged particles in Pb-Pb collisions at $\sqrt{s_{\rm NN}} = 2.76$ TeV. Phys. Lett. B **762**, 376–388 (2016). doi:10.1016/j.physletb.2016.07.017

[55] S. Acharya, D. Adamová, A. Adler, et al., Probing the effects of strong electromagnetic fields with charge-dependent directed flow in Pb-Pb collisions at the LHC. Phys. Rev. Lett. **125**, 022301 (2020). doi:10.1103/PhysRevLett.125.022301

ChinaXiv合作期刊

[56] S.K. Das, S. Plumari, S. Chatterjee, et al., Directed Flow of Charm Quarks as a Witness of the Initial Strong Magnetic Field in Ultra-Relativistic Heavy Ion Collisions. Phys. Lett. B **768**, 260–264 (2017). doi:10.1016/j.physletb.2017.02.046

[57] U. Gürsoy, D. Kharzeev, E. Marcus, et al., Charge-dependent Flow Induced by Magnetic and Electric Fields in Heavy Ion Collisions. Phys. Rev. C **98**, 055201 (2018). doi:10.1103/PhysRevC.98.055201

[58] S. Chatterjee, P. Bożek, Large directed flow of open charm mesons probes the three dimensional distribution of matter in heavy ion collisions. Phys. Rev. Lett. **120**, 192301 (2018). doi:10.1103/PhysRevLett.120.192301

[59] J. Adam, et al., First Observation of the Directed Flow of D^0 and $\overline{D^0}$ in Au+Au Collisions at $\sqrt{s_{\rm NN}}$ = 200 GeV. Phys. Rev. Lett. **123**, 162301 (2019). doi:10.1103/PhysRevLett.123.162301

[60] A.M. Sirunyan, et al., Measurement of prompt $\rm D^0$ and $\overline{\rm D}^0$ meson azimuthal anisotropy and search for strong electric fields in PbPb collisions at $\sqrt{s_{\rm NN}}$ = 5.02 TeV. Phys. Lett. B **816**, 136253 (2021). doi:10.1016/j.physletb.2021.136253

chinaXiv:202201.00065v1